

## Preparation of heterogeneous Fenton catalyst Fe/organo-attapulгите and its performance in sodium humate degradation

Ting Zhang\*, Jin Liu, Minmin Chen, Yi Wang

Department of Petrochemical Engineering, Lanzhou University of Technology, Lanzhou, 730050, China, Tel. +86-931-7823126, email: zhangting@lut.cn (T. Zhang), 920659418@qq.com (J. Liu), 2550347292@qq.com (M. Chen), wangyi@lut.cn (Y. Wang)

Received 30 August 2017; Accepted 23 February 2018

### ABSTRACT

A novel heterogeneous Fenton catalyst Fe/organo-attapulгите (Fe/OATP) was prepared by introducing nano-Fe into organic modified attapulгите with redox method. The new catalyst was characterized by XRD, IR and SEM, and a series of experiments were conducted for investigating the influences of pH value, catalyst dosage, hydrogen peroxide concentration, reaction temperature and initial concentration of HA-Na solution on the degradation ratios of HA-Na in Fe/OATP/H<sub>2</sub>O<sub>2</sub> heterogeneous Fenton system. Through a number of degradation experiments under various conditions, the results showed that the removal ratio of HA-Na can reach more than 97% at the condition of pH value 8, the reaction temperature 70°C, the initial HA-Na concentration 100 mg/L, the catalysts dosage 10 g/L, and the H<sub>2</sub>O<sub>2</sub> concentration 78.4 mmol/L. According to the results of dynamics experiments, the degradation of HA-Na followed the first-order kinetics. Fe/OATP catalyst has a wide pH range in heterogeneous Fenton reaction and can be reused for many runs with good capacity of HA-Na degradation.

*Keywords:* Attapulгите (ATP); Heterogeneous Fenton catalyst; Degradation; HA-Na

### 1. Introduction

Humic substances are the final products of animals and plants remains decomposed by microbial and chemical processes. Humic substances cause pollution of the surface water and groundwater [1] for its brown or yellowish color and bad smell. Humic substances, important precursors of chlorinated disinfection by-products [2], are widely found in natural water. Although they have no mutagenicity, they will contribute to form harmful substances that may lead to potential carcinogenesis, teratogenesis and mutagenesis during the process of chlorination disinfection. On the other hand, humic substances have the strong adsorption capacity of heavy metals and have serious effect on the transformation and migration of heavy metals in water. Some researchers used humic acid as an absorbent for removing heavy metals from wastewater. There are some methods of humic substances removal from water, including activated carbon adsorption [3,4], enhanced coagulation [5,6], ozone

oxidation [7,8], intensified ozonation [9,10], photo catalytic oxidation [11–13], biological fluidized bed [14], etc. Fenton oxidation method has been widely studied due to its simple reaction and low cost [15]. In homogeneous Fenton process, active ·OH radicals produced by the reaction between hydrogen peroxide and dissolved ferrous ions have strong oxidation degradation ability to oxidize the organic compounds in wastewater to purified water. Furthermore, heterogeneous Fenton reactions on solid catalysts can effectively catalyze the oxidation of organic pollutants at wide pH conditions, and can be reused for further runs [16–20]. In many Fenton processes associated with humic acid, researchers often use humic acid (HA) as an assistant agent to remove other organics which are hard to degrade [21–23], but Fenton methods (homogeneous or heterogeneous Fenton methods) were seldom used for humic substances removal. Only a few researches involved humic substances removal by Fenton methods but these methods still have some defects. For instance, iron oxides coated on Fe<sup>0</sup> core-shell nano spheres (nIOCI) were synthesized [24] and the catalyst was highly effective for the degradation of humic

\*Corresponding author.

acid (HA) in the presence of  $H_2O_2$  and UVA at neutral pH, while the catalyst is nano spheres which is hard to separate or recycle, and the HA removal experiments must be carried out in the presence of UVA. Another example is that Trellu et al. [25] used electro-Fenton (EF) for the removal of humic acids (HAs) from aqueous solutions. Electro-Fenton (EF) still belongs to homogeneous Fenton methods having the drawbacks of tight pH range and hard-to-separate ferric ions. Although Fenton process has emerged as one of the most promising alternative strategies for wastewater treatment, unfortunately, it is still challenging to deal with iron sludge generated during the process, which is of great importance for practical application [26].

Clays such as montmorillonite, kaoline, attapulgite, are often used as support of heterogeneous catalysts to lower the wastewater treatment cost. Attapulgite is a crystalline hydrated magnesium aluminum silicate and has a fibrous morphology. Due to its unique three-dimensional structure, attapulgite has received considerable attention to the adsorption of organics on its surface and to the support for catalysts [27]. Zhang and Nan [16] have synthesized a kind of heterogeneous Fenton catalyst ( $Fe_2O_3/ATP$ ) which was used to degrade MB and CR dye and gained almost 100% decolorization ratios under optimized conditions. In order to improve the inter facial interaction and obtain a better compatibility with organic molecules, it is necessary to modify attapulgite organically. For instance, Zhang et al. [28] modified attapulgite by CATB and synthesized  $Cu/TiO_2$ /organo-attapulgite fiber nano composite for degradation of acetone in air. Wang and Sheng [29] modified attapulgite by silane coupling agent and butyl acrylate, prepared polypropylene/org-attapulgite nano composites and tested its properties.

Referring to the above mentioned heterogeneous Fenton methods applications, this study aimed to remove humic substances by Fe-coated clay-based catalysts on heterogeneous Fenton methods. To fulfill that purpose, we considered (i) to synthesize a new nano Fe-coated attapulgite-based catalyst, (ii) to apply Fe-coated attapulgite-based catalyst on humic substances removal (e.g. HA-Na), and (iii) to optimize the experimental conditions of removal HA-Na by prepared catalyst in presence of  $H_2O_2$ .

With this respect, ATP modified by organics was used as a supporter to prepare a new heterogeneous catalyst Fe/OATP by redox method. The effects of pH, dosage of catalyst, concentration of hydrogen peroxide, temperature and initial concentration of HA-Na on HA-Na removal ratio were investigated. And the kinetics of the heterogeneous Fenton reaction and reusability of the catalyst were also discussed.

## 2. Experimental

### 2.1. Materials

Attapulgite (ATP), as carrier without further purification, was obtained from Xuyi County, Jiangsu Province, China.  $H_2O_2$  (30%), HCl,  $AgNO_3$ ,  $C_{21}H_{46}NCl$ ,  $C_2H_5OH$ ,  $FeSO_4 \cdot 7H_2O$ ,  $NaBH_4$  were supplied by chemical reagent companies and all of them were analytical grade. Distilled water used throughout the experiments was self-made by our laboratory.

### 2.2. Characterization

A field-emission scanning electron microscope (JSM-6701, JEOL Ltd., Japan) was used to characterize the surface morphologies of the samples in room temperature at an acceleration voltage of 20 kV. Before the investigation, all samples were dispersed in ethanol by ultra sonicator (Kunshan, KQ3200DE, China), and they were prepared to be electrically conductive by sputter coating with a thin layer of gold in vacuum conditions to avoid charge accumulations. A FT-IR spectroscope (Nicolet AVTAR 360, Thermo Electron Corp., U.S.A) with a KBr disk was used to examined chemical structure and any changes in the compositional or functional groups during the preparation of the samples in the range of  $4000-400\text{ cm}^{-1}$  at room temperature. To investigate the crystalline structure and stability of ATP, OATP and Fe/OATP composites, powder X-ray diffraction patterns were recorded by X-ray diffractometer (XRD-6000, SHIMADZU Ltd., Japan) using  $Cu\ K\alpha$  radiation ( $\lambda = 0.1542\text{ nm}$ ) at a rate of  $4^\circ/\text{min}$  in the range of  $2-80^\circ$ .

### 2.3. Fe/OATP catalyst preparation

Attapulgite (ATP) was firstly acidified with 1 mol/L of HCl solution, then washed with distilled water for three times and dried at  $110^\circ\text{C}$  for 2 h. Octadecyltrimethyl ammonium chloride (OATC) was weighed according to a certain proportion (30 mmol OTAC/100g  $H_2O$ ), and dissolved in 50 mL of distilled water. Then 5 g of acidified ATP was added into the OATC solution at  $60^\circ\text{C}$ . The mixture was stirred for 1 min, and treated in an ultrasonic instrument for 15 min. After that, the clay was washed with distilled water for three times, and dried in vacuum at  $110^\circ\text{C}$  to obtain the organo-modified attapulgite (OATP).

3 g of OATP and 3.72 g of  $FeSO_4 \cdot 7H_2O$  were weighed and put into a beaker which contained 200 mL distilled water, then stirred constantly the hybrid system for 6 h at room temperature. 1.517 g of sodium borohydride ( $NaBH_4$ ) was slowly put into the beaker and stirred constantly for 30 min. At the same time, a large number of black floccules were produced. The black floccules were filtered and washed with ethanol for at least three times, and dried in a vacuum drying oven at  $60^\circ\text{C}$  for 2 h to obtain the catalyst Fe/OATP. The synthesis process of Fe/OATP can be seen in Fig. 1.

### 2.4. Degradation method of HA-Na by Fe/OATP/ $H_2O_2$ system

1000 mg/L HA-Na was prepared using distilled water as a stock solution, subsequently diluted to the needed concentration for the experimental work. And 100 mg/L HA-Na solution was obtained by putting 90 mL distilled water and 10 mL HA-Na solution (1000 mg/L) together in a conical flask. The pH was adjusted by addition of NaOH (0.1 mol/L) or  $H_2SO_4$  (0.1 mol/L) to the HA-Na solutions. Then, Fe/OATP catalyst samples were put into the conical flask containing 100 mL HA-Na solution (100 mg/L), and required dosage hydrogen peroxide (30% w/w) was also added in. The conical flasks were sealed and placed in a constant-temperature water-bath at a certain temperature. An AOE 9000 type ultraviolet-visible spectrophotometer was used to measure the HA-Na concentration by HA-Na

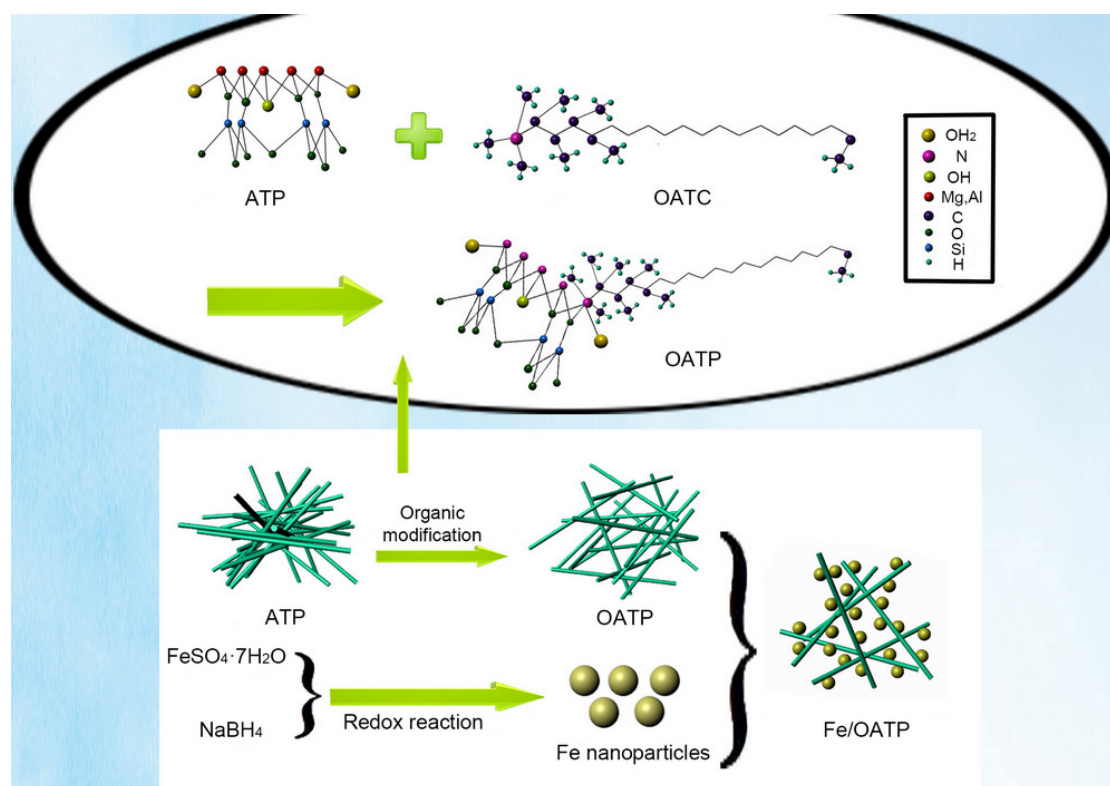


Fig. 1. Synthesis process of Fe/OATP.

spectrophotometry at  $\lambda$  of 235 nm. The degradation ratio can be calculated by the following equation:

$$\eta = (C_0 - C_t) / C_0 \times 100\% \quad (1)$$

where  $C_0$  is the initial concentration of HA-Na solution and  $C_t$  is the concentration at contact time  $t$ .

### 2.5. Measurement of $\cdot\text{OH}$ concentration

$\cdot\text{OH}$  will react with salicylic acid to produce a chemical substance called 2,3-dihydroxybenzoic acid with maximum absorption peak at the wavelength of 510 nm. 100 mL salicylic acid standard solution was put into a 250 mL conical flask, after adding 1 g heterogeneous catalyst and 0.8 mL 30%  $\text{H}_2\text{O}_2$ , the conical bottle was placed in a water bath under  $70^\circ\text{C}$ . Every 10 min the  $\cdot\text{OH}$  concentration of the solution was measured by the AOE 9000 type ultraviolet-visible spectrophotometer with spectrophotometry at  $\lambda$  of 510 nm.

## 3. Results and discussion

### 3.1. Characterization of the Fe/OATP catalyst

SEM micro graphs were collected to illustrate the morphologies of ATP, OATP, and Fe/OATP samples, as depicted in Fig. 2. As can be seen in Fig. 2a, attapulgite clay has layered and rod-like fiber structure, and the rod-like fibers of ATP intersected with each other, which

forms the porous surface, so that the ATP particles have high surface area and high absorption capacity. From Fig. 2b we can see that the length of the rod crystal have no big change after modification, but the layered structure, the surface area and pore volume of the particles increase significantly, which means that the organic modification successfully enlarge the specific surface area of the ATP particles. After introducing nano-Fe into modified ATP particles, as shown in Fig. 2c, the spherical material with a diameter of about 80 nm is on the rod structure of OATP, which shows that the nano iron is loaded on the structure of OATP successfully.

The FT-IR results of ATP, OATP, and Fe/OATP samples are shown in Fig. 3. The broad absorption bands at  $3850\text{ cm}^{-1}$  and  $3500\text{ cm}^{-1}$  are characteristics of the stretching vibration of surface hydroxyl ( $-\text{OH}$ ) groups. The strong wide absorption bands at  $1020\text{ cm}^{-1}$  is the stretching vibrations of Si-O bonds and the weak peak at  $1650\text{ cm}^{-1}$  is the bending vibration absorption peak of water (H-O-H) group. The peak at  $1460\text{ cm}^{-1}$  is the C-H bending vibration of  $-\text{CH}_3$ . The absorption bands at  $833\text{ cm}^{-1}$  and  $498\text{ cm}^{-1}$  are characteristics peaks of the typical ATP. Some peaks observed at  $2923\text{ cm}^{-1}$  and  $2850\text{ cm}^{-1}$  in FT-IR curves of samples OATP and Fe/OATP, are symmetric stretching vibration peaks of  $-\text{CH}_3$  and  $-\text{CH}_2$ , respectively. These peaks indicate that attapulgite clay is successfully modified by organics. After introducing the Fe species, the peaks at  $2923\text{ cm}^{-1}$  and  $2850\text{ cm}^{-1}$  become weak.

The phase structures of samples were investigated by XRD, and the obtained results of the ATP, OATP, and Fe/OATP samples are shown in Fig. 4. The strong peaks at  $5.3^\circ$ ,  $19.7^\circ$ ,  $34.6^\circ$ ,  $35.2^\circ$ ,  $42.6^\circ$  and  $78.7^\circ$  could be found in

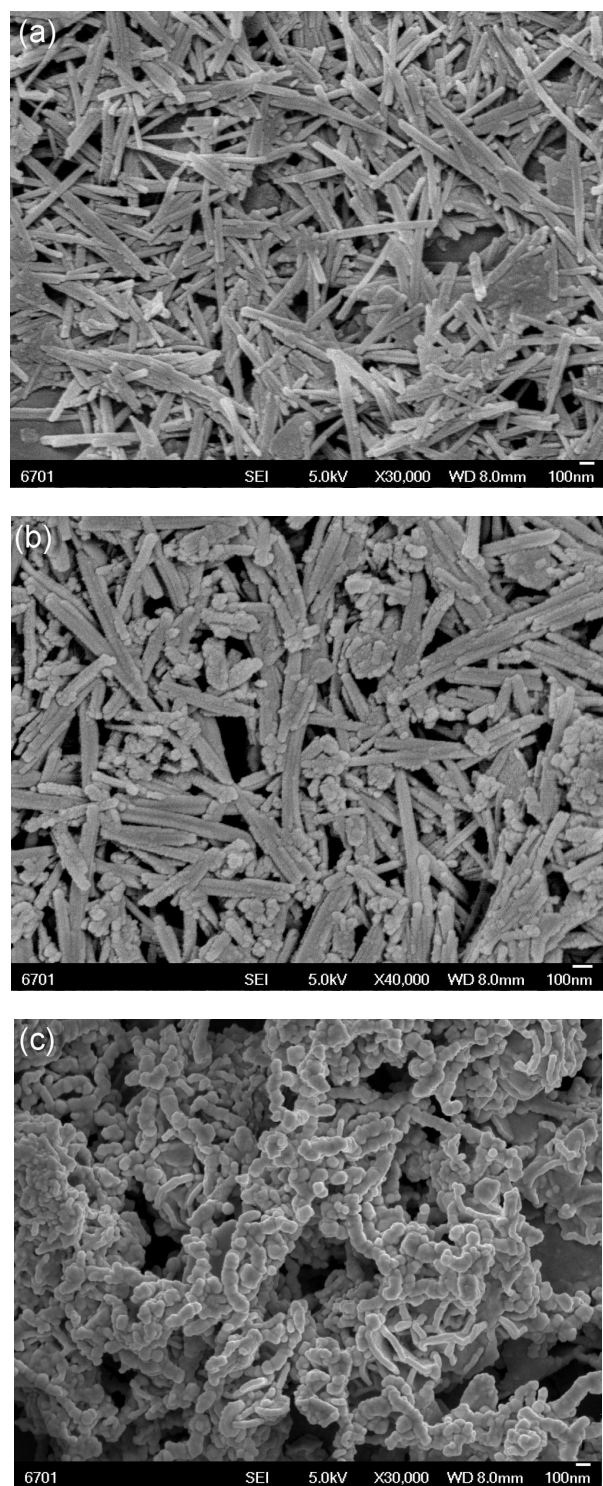


Fig. 2. SEM images of the samples (a) ATP (b) OATP (c) Fe/OATP.

the XRD patterns of all these three samples, which means the crystal structure of ATP has not been broken during the process of modification or preparation. The characteristic peaks at  $50.4^\circ$ ,  $61.9^\circ$ ,  $73.14^\circ$  shown in sample of Fe/OATP indicates that Fe<sup>0</sup> was successfully located on the clay structure.

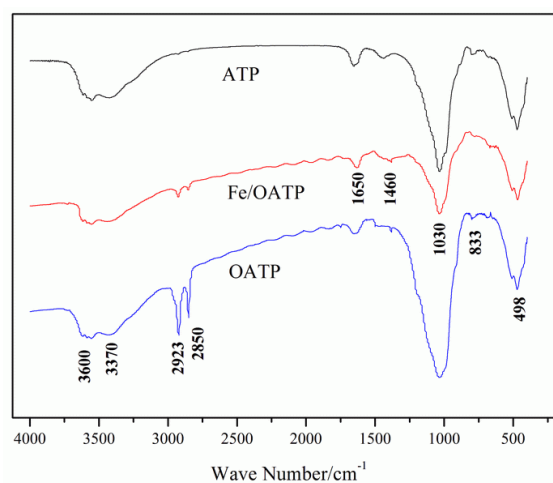


Fig. 3. FT-IR spectroscopies of the samples (ATP, OATP and Fe/OATP).

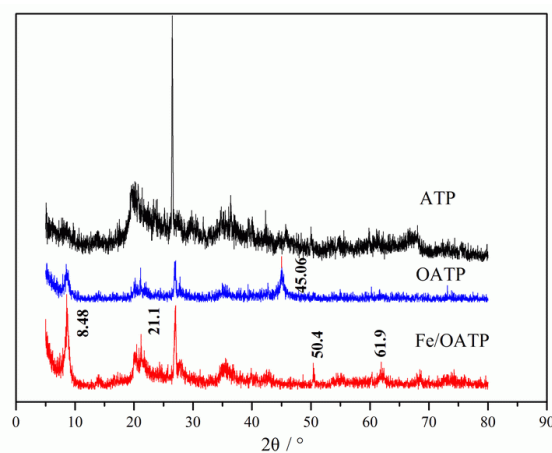


Fig. 4. XRD patterns of the samples (ATP, OATP and Fe/OATP).

### 3.2. Degradation of HA-Na by Fe/OATP/H<sub>2</sub>O<sub>2</sub> system

In order to optimize the catalytic performance of degradation of HA-Na by Fe/OATP/H<sub>2</sub>O<sub>2</sub> heterogeneous Fenton system, a series of single factor experiments were carried out, and the influences of pH value, reaction temperature, catalyst dosage and H<sub>2</sub>O<sub>2</sub> dosage on degradation of HA-Na were studied.

The effect of pH value on the degradation of HA-Na is shown in Fig. 5. At acidic condition, HA-Na no longer exists and it is replaced by HA, which is insoluble in water and easy to separate from water. So, the experimental pH values were chosen to be 7, 8, 9, 10 and 11, under which condition HA exists in the form of soluble HA-Na. Under different initial pH value, the degradation ratio of HA-Na increased with the growth of reaction time in catalytic degradation process. When the initial pH values were 7, 8, 9, 10 and 11, after 60 min reaction the degradation ratios of HA-Na were 91.4%, 96.3%, 90.4%, 94.3% and 87.0% respectively. It can be concluded that the degradation ratio of HA-Na was the highest at pH value of 8. At the same time the degradation

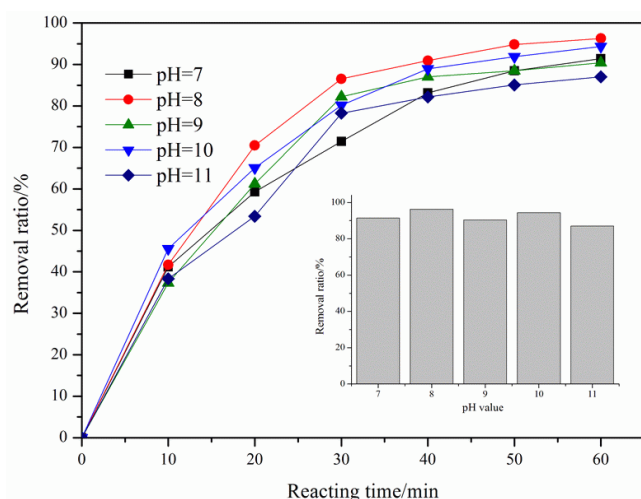


Fig. 5. Influences of pH value on HA-Na removal ratio at initial HA-Na concentration 100 mg/L, catalyst dosage 10 g/L,  $H_2O_2$  dosage 98 mmol/L and reaction temperature 60°C.

ratios of HA-Na reached over 85% under all experimental pH values. The results suggest that the catalyst (Fe/OATP) can overcome the drawback of a narrow pH range of heterogeneous Fenton reaction [30] and extend the pH range to the alkaline zone. The pH value affects the surface characteristics of the catalysts, particularly affects the surface electric charge which has important effect on their adsorption capacity towards organic molecules and their intermediate products. As can be seen from Fig. 5, with the increase of pH, the ratio of degradation of HA-Na basically increased first and then decreased, but rose up again at pH 10. This may be because  $H_2O_2$  could be catalyzed to generate  $\cdot OH$ , or directly decompose to  $HOO^-$  and  $H^+$ , depending on different pH value. For example, the formation rate of  $\cdot OH$  is the highest at pH 8, so that the degradation ratio is also highest. With the pH increasing, the amount of  $OH^-$  in the solution increases as well, which facilitates active component peroxy hydroxyl ion ( $HOO^-$ ) generating, but  $\cdot OH$  concentration decreases. When pH increases to 10, due to formation of a large amount of  $HOO^-$ , under the synergistic effects of  $\cdot OH$  and  $HOO^-$ , the degradation ratio rises again. Moreover, a further rise of pH value leads to increase the coulombic repulsion between the negative charged catalyst surface (Fe/OATP) and the  $HA^-$ , which makes adsorption of the catalyst decrease, and subsequently catalysis capacity decreases. And the higher the pH value is, the bigger the coulombic repulsion is [31].

To evaluate the influence of reaction temperature on the degradation of HA-Na in this heterogeneous Fenton system, a series of experiments were performed under the reaction temperature of 30°C, 40°C, 50°C, 60°C and 70°C. As shown in Fig. 6, under different reaction temperature, the HA-Na degradation ratios increase with the growth of reaction temperatures. When the reaction temperatures are 30°C, 40°C, 50°C, 60°C and 70°C, after 60 min reaction, the degradation ratios are 71.4%, 90.0%, 90.9%, 95.3%, and 97.3%, respectively. It is obviously shown that the degradation ratio of HA-Na is the highest under the reaction temperature of 70°C, because the number of  $\cdot OH$  radicals boosts at a higher

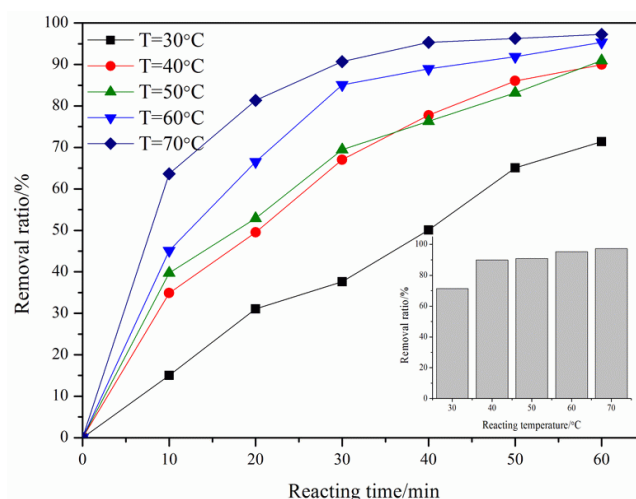


Fig. 6. Influences of reaction temperature on HA-Na removal ratio at initial HA-Na concentration 100 mg/L, catalyst dosage 10 g/L,  $H_2O_2$  dosage 98 mmol/L and pH 8.

temperature and leads a faster catalysis to decompose  $H_2O_2$ . Another reason is that higher temperature can supply more energy for reactant molecules to overcome reaction activation energy. The activation energy in this catalytic reaction is calculated to be 64.74 kJ/mol, which is not very high and easy to overcome by increasing the reaction temperature. But the reaction temperature should not be too high due to poor stability of  $H_2O_2$ .  $H_2O_2$  can be decomposed into  $H_2O$  and  $O_2$  at high temperature and consumed ineffectively. Furthermore, evaporation rate of water is high because of high reaction temperature, the solution will be concentrated and the results deviation will occur. To avoid decomposition and deviation, the experimental temperature should not exceed 60°C.

Fig. 7 shows HA-Na degradation ratios versus different catalyst dosages changing from 2 g/L to 10 g/L. The data indicate that degradation ratio of HA-Na increases with increasing catalyst dosage. When catalyst dosage increases from 2 g/L to 10 g/L, the removal ratio rises from 72.4% to 96.8%. The results suggest that the more catalysts are, the more active Fe sites on catalyst surface are, leading to an increase in the number of OH radicals.

The concentration of  $H_2O_2$  plays an important role in removal ratio of HA-Na. The effect of  $H_2O_2$  concentration on the degradation of HA-Na was examined under various  $H_2O_2$  dosages. The results are presented in Fig. 8. It can be seen that the degradation ratio of HA-Na ascends with the increase of  $H_2O_2$  concentration. The degradation ratio of HA-Na rises from 88.1% to 97.3% with the increase of  $H_2O_2$  concentration from 19.6 mmol/L to 78.4 mmol/L, then went down to 95.3% at 98 mmol/L. These results can be attributed to more OH radicals producing with the increase of  $H_2O_2$  dosage, which dramatically enhances the degradation ratio of HA-Na [32]. However, too more  $H_2O_2$  will react with OH radicals and release oxygen. The reactions are as follows [33]:



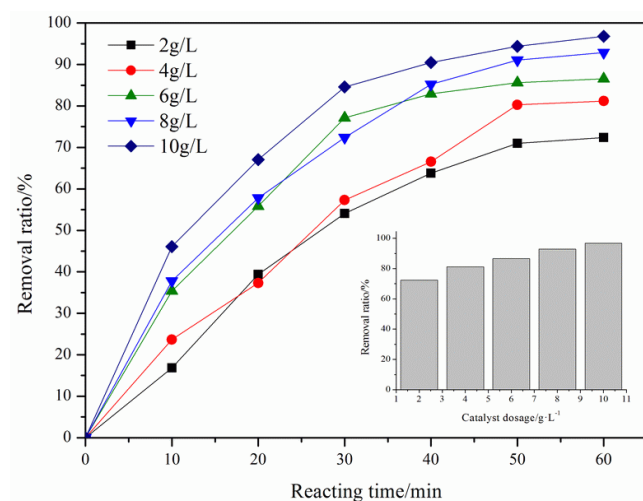


Fig. 7. Influences of catalysts dosage on HA-Na removal ratio at initial HA-Na concentration 100 mg/L, pH 8,  $H_2O_2$  dosage 98 mmol/L and reaction temperature 60°C.

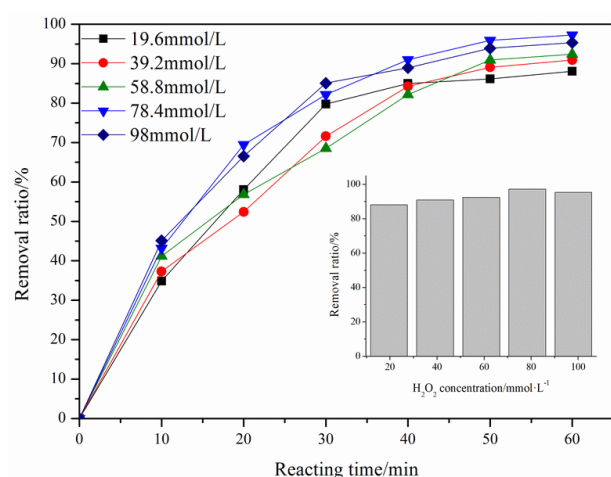


Fig. 8. Influences of  $H_2O_2$  concentration on HA-Na removal ratio at initial HA-Na concentration 100 mg/L, pH 8, catalyst dosage 10 g/L and reaction temperature 60°C.

To get a clear understanding of the HA-Na degradation process by Fe/OATP/ $H_2O_2$  system, comparison experiments about the degradation experiments were conducted with  $H_2O_2$ , Fe/OATP and Fe/OATP/ $H_2O_2$  separately. The results are shown in Fig. 9. Fig. 9a shows that the degradation ratio of HA-Na is not very high when only  $H_2O_2$  exists and obtains 40% degradation ratio after 60 min, which means that HA-Na can be oxidised by  $H_2O_2$  gradually. When only Fe/OATP exists, the degradation ratio of HA-Na can reach over 30% after 60 min due to the adsorptive ability of Fe/OATP. It also can be seen that after organic modification of ATP, the adsorption ability of OATP rises a lot contrasted with its original form (Fig. 9b). When both Fe/OATP and  $H_2O_2$  exist, the degradation ratio of HA-Na can reach 99% within 60 min, as depicted in Fig. 9c. It implies that in Fe/OATP/ $H_2O_2$  system, the catalytic degradation reaction is the main reaction in HA-Na degradation process other than directly oxidation by  $H_2O_2$  or adsorption by Fe/OATP.

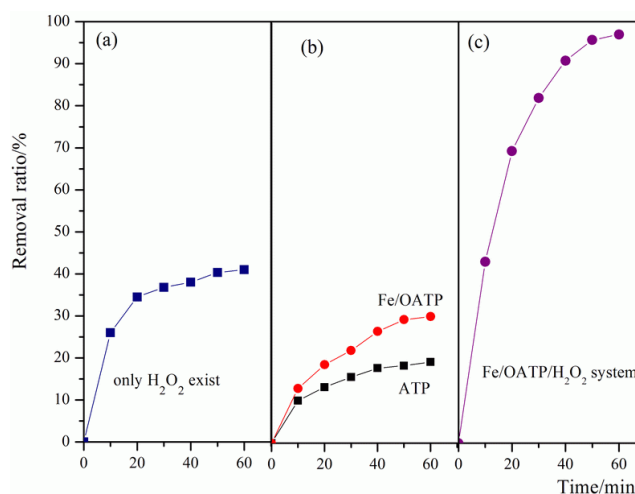
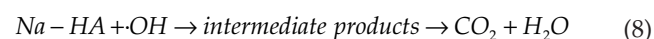
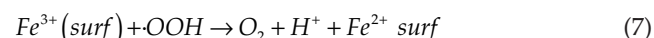
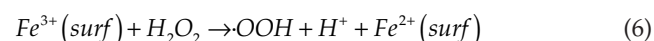
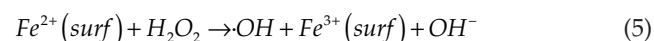
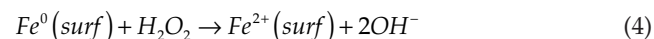


Fig. 9. Comparison experiments in the presence of (a) only  $H_2O_2$  exist (b) only Fe/OATP or only ATP exist (c) Fe/OATP/ $H_2O_2$  system.

### 3.3. Mechanism of the degradation of HA-Na by Fe/OATP/ $H_2O_2$ heterogeneous Fenton system

The  $\cdot OH$  trapping experiments were also carried out to prove that HA-Na degradation reaction is a heterogeneous Fenton process. The  $\cdot OH$  trapping experiments were conducted under the optimized condition of pH 8, reaction temperature 70°C, the catalysts dosage 10 g/L, and the  $H_2O_2$  dosage 78.4 mmol/L, and the  $\cdot OH$  concentration produced in the reaction at different times were measured, shown in Fig. 10. As can be seen that with the reaction time increases, the  $\cdot OH$  concentration increases accordingly, and the  $\cdot OH$  concentration is pretty high, which can demonstrate that the degradation reaction is a Fenton process.

A possible mechanism for the degradation of HA-Na by Fe/OATP/ $H_2O_2$  system was proposed.  $Fe^0$  immobilized on the heterogeneous catalyst surface is the active component reacting with  $H_2O_2$ . During the reaction, immobilized  $Fe^{2+}$  is produced and reacted with adsorbed  $H_2O_2$  to generate  $\cdot OH$  and oxidize HA-Na to simple organics or even  $H_2O$  and  $CO_2$ . The reaction equations are as follows:



### 3.4. Study on degradation kinetics

In order to study the dynamic of HA-Na removal in the heterogeneous Fenton system, the changes of concentration were tested during the process (0–60 min) which used Fe/

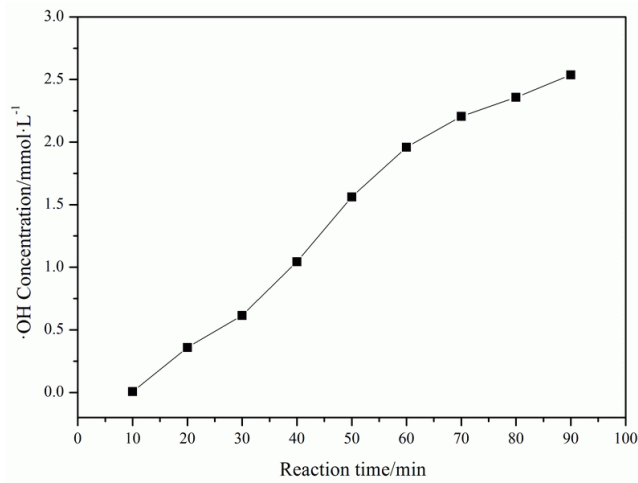


Fig. 10. Production of OH radicals under the optimized condition (pH 8, reaction temperature 70°C, initial HA-Na concentration 100 mg/L, the catalysts dosage 10 g/L, and the H<sub>2</sub>O<sub>2</sub> dosage 78.4 mmol/L).

OATP as catalyst, and the initial HA-Na concentration were varying from 50 mg/L to 250 mg/L, as shown in Fig. 11. The concentration of HA-Na drops sharply under higher initial HA-Na concentration while it drops steadily under low concentration.

First-order kinetic model was used to fit the kinetics formula of the HA-Na oxidation by hydroxyl radicals,

$$\ln\left(\frac{C_0}{C}\right) = kt \quad (9)$$

which was contrasted with second-order kinetic model:

$$\frac{1}{C} - \frac{1}{C_0} = kt \quad (10)$$

where  $C$  is the concentration of the HA-Na (mg/L) at reaction time  $t$ ,  $C_0$  is the initial concentration of HA-Na (mg/L),  $t$  is the reaction time for degradation of HA-Na, and  $k$  is the constant of the action.

The fitting results of various kinetic models are shown in Table 1.

Compared to second-order kinetics model, as shown in Table 1, the first-order kinetics model is more appropriate for the heterogeneous Fenton degradation process by using Fe/OATP as catalyst, because under different initial concentration, all fitting models show good linear correlation ( $R^2 > 0.98$ ).

### 3.5. Stability and reusability of catalysts

The repeatable use of the catalysts was also tested through the experiments, which were carried out in ten consecutive runs under the same conditions (Initial HA-Na concentration of 100 mg/L, catalyst dosage of 10 g/L, H<sub>2</sub>O<sub>2</sub> dosage of 78.4 mmol/L, reaction temperature of 60°C and pH value of 8). After reaction at each run, the catalysts used in the experiments were just washed with distilled water. According to the experiments, it is found that after ten runs of reactions by recycled catalysts, HA-Na degradation retain a high efficiency (Fig. 12). What's more, the

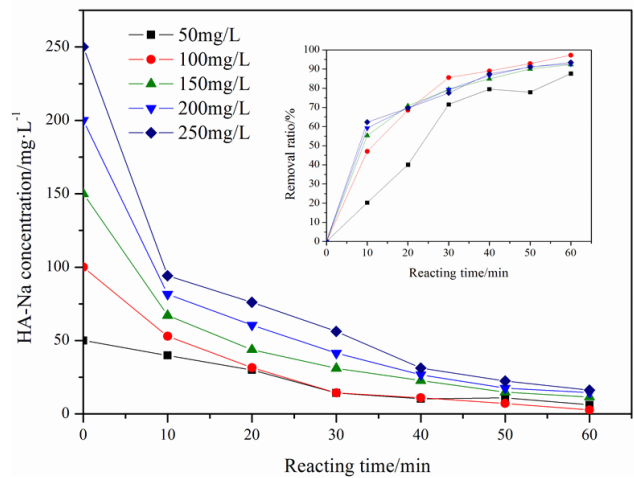


Fig. 11. Degradation of HA-Na at different initial concentration.

Table 1  
Fitting results using different kinetic models

Kinetic model	Fitting formula	$C_0$	$k$	$V_0$	$R^2$
First-order	$\ln\left(\frac{C_0}{C}\right) = kt$	50	0.03459	0.00765	0.98019
		100	0.05755	0.02546	0.99471
		150	0.04669	0.03099	0.98274
		200	0.04827	0.04272	0.98183
		250	0.04903	0.05424	0.98170
Second-order	$\frac{1}{C} - \frac{1}{C_0} = kt$	50	0.00187	0.00041	0.92144
		100	0.00366	0.00162	0.75471
		150	0.00115	0.00076	0.96683
		200	0.00094	0.00083	0.96560
		250	0.00080	0.00089	0.94798

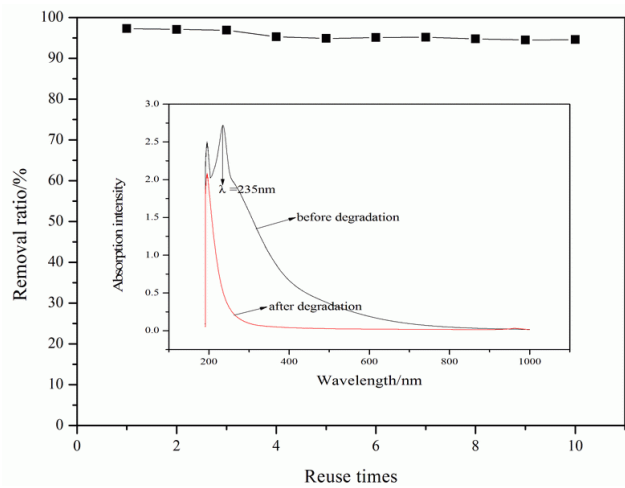


Fig. 12. Ten repeated runs at initial HA-Na concentration 100 mg/L, catalyst dosage 10 g/L, H<sub>2</sub>O<sub>2</sub> concentration 78.4 mmol/L, reaction temperature 60°C, pH 8 and reacting time 60 min.

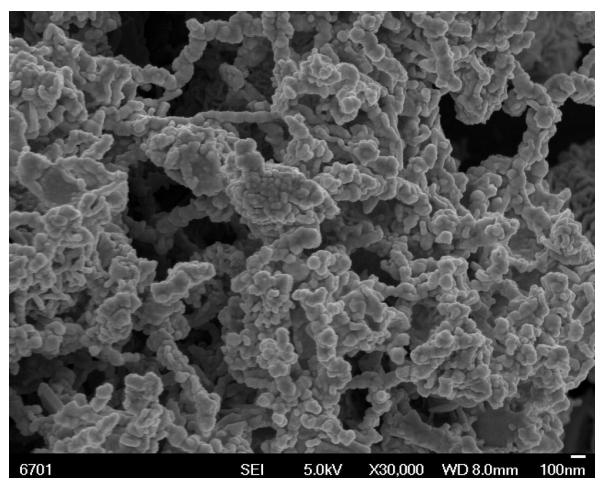


Fig. 13. The SEM image of the catalyst after ten runs of HA-Na degradation.

leaching iron ion concentration is tested to be  $5.95 \times 10^{-3}$  mg/L, which can almost be ignored. Under such low free iron ion concentration, the catalytic reaction hardly can be conducted in homogeneous Fenton system. That indicates Fe/OATP/H<sub>2</sub>O<sub>2</sub> system is surely a heterogeneous system and the catalyst has a strong stability. And the SEM image about the catalyst after ten runs is shown in Fig. 13. It is almost the same condition of that before used. As a result, the catalyst is stable and reusable.

The full-wave band ultraviolet scanning of the aqueous solution containing HA-Na before and after degradation in Fe/OATP/H<sub>2</sub>O<sub>2</sub> system are also shown in Fig. 12. It can be seen that the absorption peak at 235 nm of HA-Na disappeared after degradation, without the appearance of new adsorption peaks.

#### 4. Conclusions

Heterogeneous catalyst (Fe/OATP) which used organic modified attapulgite as a carrier were successfully prepared by redox method. SEM, XRD, FT-IR were used to characterize the structure of catalyst. The results showed that the inter space among the rod-like crystal fibers was broadened, and nano Fe<sup>0</sup> was loaded on the surface of their rod structure. Through a series of experiments, it was found that the removal ratio of HA-Na can reach more than 97% after 60 min reaction under the optimized condition of pH 8, reaction temperature 70°C, initial HA-Na concentration 100 mg/L, the catalysts dosage 10 g/L, and the H<sub>2</sub>O<sub>2</sub> dosage 78.4 mmol/L. Kinetic experiments demonstrated that the degradation of HA-Na followed a first-order kinetic. The repeatable tests showed that the Fe/OATP catalyst can be reused for many times, which meets the trend of low carbon life style. The research provided a new and effective method for the humic acid removal in the micro polluted water source.

#### Acknowledgment

This work was financially supported by the National Natural Science Foundation of China (Grant No. 51302123).

#### References

- [1] A.A. Helal, G.A. Murad, A.A. Helal, Characterization of different humic materials by various analytical techniques, *Arab. J. Chem.*, 4 (2011) 51–54.
- [2] W.S.W. Ngah, S. Fatinathan, N.A. Yosop, Isotherm and kinetic studies on the adsorption of humic acid onto chitosan-H<sub>2</sub>SO<sub>4</sub> beads, *Desalination*, 272 (2011) 293–300.
- [3] Q.Y. Yue, J.K. Xie, B.Y. Gao, H. Yu, W.W. Yue, S.X. Zhang, X.N. Wang, Kinetics of adsorption of dyes by sludge activated carbon, *Acta Sci. Circumst.*, 27 (2007) 1431–1438.
- [4] J.E. Kilduff, T. Karanfil, W.J. Weber, Competitive interactions among components of humic acids in granular activated carbon adsorption system: effects of solution chemistry, *Environ. Sci. Technol.*, 30 (1996) 1344–1351.
- [5] J. Duan, J. Wang, N. Graham, F. Wilson, Coagulation of humic acid by aluminum sulphate in saline water conditions, *Desalination*, 150 (2001) 1–14.
- [6] H.J. Liu, R.P. Liu, C. Tian, H. Jiang, X. Liu, Removal of natural organic matter for controlling disinfection by-products formation by enhanced coagulation, *Sep. Sci. Technol.*, 84 (2012) 41–45.
- [7] H. Miao, W. Tao, F. Cui, Z. Xu, Z. Ao, Kinetic Study of Humic Acid Ozonation in Aqueous Media, *Clean*, 36 (2008) 893–899.
- [8] V.V. Tarasov, Linearization of kinetic curves of the ozonation of dyes and humic acids, *Theor. Found. Chem. Eng.*, 42 (2008) 530–535.
- [9] D. Gümüs, F. Akbal, A comparative study of ozonation, iron coated zeolite catalyzed ozonation and granular activated carbon catalyzed ozonation of humic acid, *Chemosphere*, 174 (2017) 218–231.
- [10] O. Turkey, H. Inan, A. Dimoglo, Experimental and theoretical study on catalytic ozonation of humic acid by ZnO catalyst, *Sep. Sci. Technol.*, 52 (2017) 778–786.
- [11] X.Z. Li, C.M. Fan, Y.P. Sun, Enhancement of photo catalytic oxidation of humic acid in TiO<sub>2</sub> suspensions by increasing cation strength, *Chemosphere*, 48 (2002) 453–460.
- [12] J.Y. Kim, C.S. Kim, H.K. Chang, T.O. Kim, Effects of ZrO<sub>2</sub> addition on phase stability and photo catalytic activity of ZrO<sub>2</sub>/TiO<sub>2</sub> Nano particles, *Adv. Powder Technol.*, 21 (2010) 141–144.
- [13] N.C. Birben, C.S. Uyguner-Demirel, S.S. Kavurmaci, Y.Y. Gürkan, N. Turkten, Z. Cinar, M. Bekbolet, Application of Fe-doped TiO<sub>2</sub> specimens for the solar photo catalytic degradation of humic acid, *Catal. Today*, 281 (2017) 78–84.
- [14] T. Huang, X. Xiong, A dynamic model of humic acid biological degradation by biological fluidized bed, *China Environ. Sci.*, 18 (1998) 531–534.
- [15] J.A. Zazo, J.A. Casas, A.F. Mohedano, J.J. Rodriguez, Semicontinuous Fenton oxidation of phenol in aqueous solution: A kinetic study, *Water Res.*, 43 (2009) 4063–4069.
- [16] T. Zhang, Z.R. Nan, Decolorization of Methylene Blue and Congo Red by attapulgite-based heterogeneous Fenton catalyst, *Desal. Water Treat.*, 57 (2016) 4633–4640.
- [17] R. Malik, V. Chaudhary, V.K. Tomer, P.S. Rana, S.P. Nehra, S. Duhan, Visible light-driven mesoporous Au–TiO<sub>2</sub>/SiO<sub>2</sub> photo catalysts for advanced oxidation process, *Ceram. Int.*, 42 (2016) 10892–10901.
- [18] H. Guo, Z. Zheng, J. Chen, W. Weng, M. Huang, Facile template-free one-pot fabrication of TiO<sub>2</sub>@C micro spheres with high visible-light photo catalytic degradation activity, *J. Ind. Eng. Chem.*, 36 (2016) 306–313.
- [19] J. He, W.H. Ma, J.J. He, J. Zhao, J.C. Yu, Photo oxidation of azo dye in aqueous dispersions of H<sub>2</sub>O<sub>2</sub>/α-FeOOH, *Appl. Catal B-Environ.*, 39 (2002) 211–220.
- [20] R.C.C. Costa, F.C.C. Moura, J.D. Ardisson, R.M. Lago, Highly active heterogeneous Fenton-like systems based on FeO/Fe<sub>3</sub>O<sub>4</sub> composites prepared by controlled reduction of iron oxides, *Appl. Catal B-Environ.*, 83 (2008) 131–139.
- [21] A. Santos, S. Rodríguez, F. Pardo, A. Romero, Use of Fenton reagent combined with humic acids for the removal of PFOA from contaminated water, *Sci. Total Environ.*, 563–564 (2016) 657–663.

- [22] F.F. Wang, Y. Wu, Y. Gao, H. Li, Z. Chen, Effect of humic acid, oxalate and phosphate on Fenton-like oxidation of micro cystin-LR by nano scale zero-valent iron, *Sep. Purif Technol.*, 170 (2016) 337–343.
- [23] K.C. Christoforidis, M. Louloudi, Y. Deligiannakis, Effect of humic acid on chemical oxidation of organic pollutants by iron (II) and  $H_2O_2$ : A dual mechanism, *Eng. Chem.*, 3 (2015) 2991–2996.
- [24] Y.L. Nie, C. Hu, L. Zhou, J.H. Qu, Q.S. Wei, D.S. Wang, Degradation characteristics of humic acid over iron oxides/FeO core-shell nano particles with UVA/ $H_2O_2$ , *J. Hazard. Mater.*, 173 (2010) 474–479.
- [25] C. Trelu, Y. Péchaud, N. Oturan, E. Mousset, D. Huguenot, E.D.V. Hullebusch, G. Esposito, M.A. Oturan, Comparative study on the removal of humic acids from drinking water by anodic oxidation and electro-Fenton processes: Mineralization efficiency and modeling, *Appl. Catal. B-Environ.*, 194 (2016) 32–41.
- [26] S. Guo, N. Yuan, G. Zhang, J.C. Yu, Graphene modified iron sludge derived from homogeneous Fenton process as an efficient heterogeneous Fenton catalyst for degradation of organic pollutants, *Micropor. Mesopor. Mater.*, 238 (2017) 62–68.
- [27] S. Guo, G. Zhang, J. Wang, Photo-Fenton degradation of rhodamine B using  $Fe_2O_3$ -Kaolin as heterogeneous catalyst: Characterization, process optimization and mechanism, *J. Colloid Interf. Sci.*, 433 (2014) 1–8.
- [28] G. Zhang, H. Wang, S. Guo, J. Wang, J. Liu, Synthesis of Cu/ $TiO_2$ /organo-attapulgite fiber nano composite and its photo catalytic activity for degradation of acetone in air, *Appl. Surf. Sci.*, 362 (2016) 257–264.
- [29] L. Wang, J. Sheng, Preparation and properties of polypropylene/org-attapulgite nano composites, *Polymer*, 46 (2005) 6243–6249.
- [30] S. Chen, Y. Wu, G. Li, J. Wu, G. Meng, A novel strategy for preparation of an effective and stable heterogeneous photo-Fenton catalyst for the degradation of dye, *Appl. Clay Sci.*, 136 (2017) 103–111.
- [31] M. Akkari, P. Aranda, H.B. Rhaïem, A.B.H. Amara, E. Ruiz-Hitzky, ZnO/clay nano architectures: synthesis, characterization and evaluation as photo catalysts, *Appl. Clay Sci.*, 131 (2015) 131–139.
- [32] H. Fida, G. Zhang, S. Guo, A. Naeem, Heterogeneous Fenton degradation of organic dyes in batch and fixed bed using La-Fe montmorillonite as catalyst, *J. Colloid Interf. Sci.*, 490 (2017) 859–868.
- [33] Y. Wu, S. Zhou, F. Qin, K. Zheng, X. Ye, Modeling the oxidation kinetics of Fenton process on the degradation of humic acid, *J. Hazard. Mater.*, 179 (2010) 533–539.